Berenguer Betrián, R.; Sieben, JM.; Quijada Tomás, C.; Morallón, E. (2016). Electrocatalytic degradation of phenol on Pt- and Ru-doped Ti-SnO2-Sb anodes in an alkaline medium. Applied Catalysis B: Environmental. 199:394-404. doi:10.1016/j.apcatb.2016.06.038.

Electrocatalytic degradation of phenol on Pt- and Ru-doped Ti/SnO_2-Sb anodes in an alkaline medium

R. Berenguer[a], J.M. Sieben[b], C. Quijada[c], E. Morallón[a,*]

[a] Departamento de Química Física and Instituto Universitario de Materiales, Universidad de Alicante, Apartado 99, E-03080 Alicante, Spain.

[b] Instituto de Ingeniería Electroquímica y Corrosión and CONICET, Universidad Nacional del Sur, Av. Alem 1253, (B8000CPB) Bahía Blanca, Argentina.

[c] Departamento de Ingeniería Textil y Papelera, Universidat Politècnica de València, Plaza de Ferrándiz y Carbonell, E-03801 Alcoy (Alicante), Spain.

Abstract

In this work, the electrocatalytic performance of Ti/SnO_2-Sb(13-x)-Pt-Ru(x) anodes (x = 0.0, 3.25 and 9.75 at. %) towards phenolate elimination has been analyzed and compared to those of conventional Ti/RuO_2 and Ti/Co_3O_4 anodes, to evaluate their application for decontamination of concentrated alkaline phenolic wastewaters. The effects of the applied current density and the nature of the anode on the activity, kinetics and current efficiency for phenolate elimination, COD removal and benzoquinone by-product formation/degradation have been thoroughly examined. The Ti/SnO_2-Sb-Pt anode exhibits the best electroactivity, fastest kinetics and highest current efficiency among the studied anodes, but poor electrochemical stability. The introduction of small amounts of Ru (3.25-9.75 at%) brings about a slight loss of the electrocatalytic performance, but it causes a remarkable increase in the stability of the electrode. In terms of energy consumption and stability, the Ti/SnO_2-Sb(9.75)-Pt-Ru(3.25) electrode seems to be the most promising anode material for the electrochemical treatment of alkaline phenolic wastewaters. The increase in current density generally leads to significantly faster phenolate, benzoquinone and COD degradations, but with lower efficiency because of an increasing selectivity to

water oxidation. A correction of the ideal kinetic model has been proposed to predict the oxidation of organics on non-active metal oxide anodes.

Keywords: electrocatalysis, electrochemical treatment, phenol removal, tin dioxide electrodes

* Corresponding author: morallon@ua.es

1. Introduction

One of the most representative groups of priority pollutants are phenolic compounds [1,2]. Phenol and its derivatives are important precursors for the production of several chemicals and goods of high industrial relevance, like phenolic and epoxy resins; nylon and aspirin; explosives, adhesives, paper, paint, dyes, herbicides and pesticides, etc. In addition, several pharmaceutical products also contain phenol, and large amounts of phenolic wastes are obtained as by product at refineries. Phenolic compounds are carcinogenic, highly toxic and may cause death even at low doses [3]. Hence, investigation on new or improved technologies and treatments for phenol abatement is of paramount importance.

Several technologies including biological depuration [4], adsorption [5], chemical [6] and supercritical water [7] oxidations, incineration [8], photocatalytic [9] and electrochemical [10-26] degradation, etc. have been proposed for the removal of phenolic compounds in wastewater. In particular, electrochemical technologies show a unique combination of advantageous features and enormous potential for wastewater treatment [27-29]. Essentially, they can be conveniently operated in situ, at ambient temperature and pressure, with low energy consumption and short time requirements, just by using electrons as the only reagent. Moreover, these technologies can eliminate pollutants of high toxicity, and can be connected and supplied with renewable energies.

In spite of all these benefits, the efficiency of electrochemical treatments strongly depends on the nature of the electrocatalyst and concentration of pollutants [30-32]. As a consequence, the practical feasibility of electrochemical technologies for wastewater treatment demands the development of low-cost anodes with enough suitable activity and stability, and it will probably be associated to (i) on-site wastewater systems releasing more concentrated and less-fluctuating wastewaters; (ii) separation and/or pre-concentration treatments (i.e., following solvent extraction, adsorption, etc.); and/or (iii) tertiary treatments to improve the effluent quality, when necessary and the cost and efficiency are less important.

Another important parameter is the pH of the aqueous medium, which remarkably affects the degradability of pollutants, the selectivity of reactions and the stability of electrodes. In literature, most work dealing with the development and study of new electrocatalysts for the electro-oxidation of phenol tested their performance at low pollutant concentration and in acid or neutral media. However, alkaline waters containing phenols are also very important wastes. They are broadly generated for example in paper and pulp de-inking processes [1,2] or when using alkaline cleaning solutions and phenolics-containing industrial detergents [1,2,33]. Most remarkably, alkaline wastewaters streams with high concentration in phenols (500-4000 ppm) are produced by petroleum (mainly from crude desalting and fractionation; thermal, catalytic or hydro-cracking; solvent refining; drying and sweetening of fuels) [1,2,34-37] and metallurgical (coke production, blast furnaces, metal finishing) [1,2,38,39] industries.

On the other hand, alkaline conditions have been found to be advantageous for the electrochemical treatment of other pollutants accompanying phenols in water, like ammonia [40] or cyanide [41,42]. In addition, these conditions are sometimes optimum for other treatments that can be combined with the electro-oxidation one [43-47]. In particular, we have previously studied the electrochemical regeneration of activated carbon saturated with phenol, and maximum efficiencies of 90 % were achieved under alkaline medium [44,45]. Upon the course of this process, the desorbed phenolate in the recirculating solution, facing to electro-oxidation, reached a maximum concentration of 1000 ppm.

Among different candidates, tetragonal rutile-like transition metal oxides (TMOs) supported on titanium (commonly known as dimensionally stable anodes, DSAs), have been successfully applied as anodes in a number of important electrolytic processes [48,49]. The stability and electrochemical activity of these electrodes are largely determined by the nature of the active component and the pH of the used medium [13-15,23,50]. The anodes based on SnO_2-Sb show low catalytic activity for the competing oxygen evolution reaction (OER), thereby being very effective for the electro-oxidation of phenol in waste waters [10-12,15,20-21]. In fact, they are considered the most promising alternative to the more expensive and fragile boron-doped diamond (BDD) electrodes [16-19] and the more harmful,

lead-leaching, PbO_2-based ones [15]. However, SnO_2-Sb anodes suffer from a quite poor electrochemical stability in different electrolytes [51-54]. Previous studies in our research group pointed out that the introduction of small amounts of Pt (3 at%) in SnO_2-Sb anodes remarkably increased their service life [20,51,52,54] and the catalytic activity towards phenol oxidation in acid medium [21]. However, SnO_2-Sb and SnO_2-Sb-Pt anodes still showed a reduced service life in alkaline conditions [20,54].

Contrary to SnO_2-Sb-based electrodes, RuO_2-based anodes have been widely used due to their high stability [54] and good catalytic activity, even for the oxygen evolution reaction (OER) [55,56] in alkaline conditions. Although RuO_2-based anodes have excellent stability, they are less active for substrate mineralization, in part because they are more efficient in the OER, which is parasitic to substrate oxidation [30-32].

There are some papers reporting on the preparation and characterization of Ru-doped SnO_2, but only a few of them evaluated their activity in the electrochemical treatment of phenol wastewaters [13,20,22-24]. In addition, all these works dealt with acid or neutral electrolytes and low phenol concentrations (< 200 ppm), and the stability and cost of the electrodes were not considered. On the other hand, to the best of our knowledge, there are a few works on the electro-oxidation of concentrated alkaline phenolic wastewaters, independently of the nature of the used anode [25,26,42].

In previous works [54,55], various Ti/SnO_2-Sb(13-x)-Pt-Ru(x) electrodes were synthesized and characterized from structural, chemical and electrochemical points of view. It was found that the introduction of low amounts of Ru (3.25-9.75 at%) into the SnO_2 rutile-like structure leads to a three-fold increase in the service life of Ti/SnO_2-Sb-Pt electrodes in alkaline solution [54]. In the present work, the influence of the substitution of Sb by Ru in Ti/SnO_2-Sb(13-x)-Pt-Ru(x) anodes in the electro-oxidation of phenol in alkaline medium is investigated. The origin of this high pH is inherent to the industrial activity where the phenolic wastes are produced [1,2,34-39], so their treatment should be carried out under these conditions for economic and environmental reasons. The experiments were carried out in an

undivided filter-press cell under galvanostatic conditions. The electrocatalytic activity of the anodes is evaluated in terms of kinetics and current efficiency for phenol oxidation, COD removal and benzoquinone by-product formation/degradation at different current densities. In addition, the performance of the electrodes is compared with that of conventional Ti/RuO_2 and Ti/Co_3O_4 ones, which have been widely studied for alkaline conditions. Finally, an analysis in terms of energy consumption and stability, has been also done to evaluate their feasible application for decontamination of alkaline phenolic wastewaters.

2. Experimental

2.1 Preparation of the electrodes

Three types of Pt- and Ru-doped SnO_2-Sb electrodes with composition SnO_2-Sb(13-x)-Pt(3)-Ru(x) (in brackets expressed as metal atomic percentage and x = 0, 3.25 and 9.75 at. %), were prepared by thermal decomposition over a Ti expanded mesh (4 cm × 5 cm × 0.05 cm, INAGASA) following the procedure described elsewhere [54,55]. For comparison purposes, conventional RuO_2 [54,55] and Co_3O_4 [57,58] electrodes were similarly prepared. Prior to their use, the Ti mesh was degreased with acetone and etched in a boiling 10% oxalic acid solution for 1 h, and then rinsed thoroughly with distilled water. The precursor solutions with the desired nominal compositions, consisting of $SnCl_4 \cdot 5H_2O$ (Aldrich), $SbCl_3$ (Fluka), $H_2PtCl_6 \cdot 6H_2O$ (Aldrich), $RuCl_3 \cdot nH_2O$ (Aldrich) and $Co(NO_3)_2 \cdot 6H_2O$ (Aldrich) in absolute ethanol (J.T. Baker) + HCl (Merck p.a.), were spread over the Ti surface by brushing. The total metallic cation concentration of these solutions was kept constant at 0.5 molal. The solvent was dried at 70 °C and the electrodes were subsequently calcined at 400 °C for 10 min, for the thermal decomposition of the salts and metal oxide formation to be accomplished. By repeating this procedure (between 20 to 25 times), the Ti support was coated with successive layers of the oxides until oxide loadings of 1.5 to 2.0 mg cm^{-2}, as determined by weight difference, were achieved. A final annealing step was carried out for 60 min at 600 °C. In the particular case of Co_3O_4, however, both the

repeated calcination and final annealing steps were performed at 350 ºC [57,58]. Considering the density for the different mineral forms (SnO_2, RuO_2 and Co_3O_4) [54,55,57,58], the nominal thickness of the deposits was estimated to be between 2 and 3 μm. Three different anodes were prepared for each composition to ensure reproducibility. The results presented in this work correspond to average values.

2.2 Electrolysis of alkaline phenolic wastewater

The electrochemical oxidation of phenol (Ph) was carried out in an undivided filter-press cell, with a plane electrode area of 20 cm^2. In these experiments, 200 mL of 1000 ppm Ph/0.5 M NaOH solution was continuously flowed and recirculated by means of a centrifugal pump. The temperature of the experiments was maintained at 25 °C. The electro-oxidation of phenol was carried out under galvanostatic control at 0.2, 0.5, 1.0, 1.5 and 2.0 A for 24 h. A plate of stainless steel was used as the cathode in all experiments.

During the electrolytic experiments, the phenolate and p-benzoquinone concentrations, as well as the chemical oxygen demand (COD) were monitored as a function of time. For doing that, various aliquots of 20-30 μL were collected at different times and submitted to analytical determination. The residual concentration of phenolate and COD were determined by using standard photometric methods with test kits and a multifunctional Spectroquant® NOVA 60 Photometer (Merck). The phenol test is not interfered by hydroquinone, benzoquinone, catechol or oligomers, possible products of phenol electroxidation. The benzoquinone formation/degradation was followed by conventional UV-Vis absorption spectroscopy (Jasco V-670 UV-Vis-NIR spectrometer) over the wavelength range of 200-400 nm. The benzoquinone absorbance was measured from the UV-absorption band centered at 319 nm, at which no interference from phenolate or other by-products occur. These values were then converted to concentration by using the calibration plots.

3. Results and discussion

3.1. Phenol electro-oxidation performance

Figures 1 and 2 show the variation of the normalized phenol concentration with time at various current densities for the as-prepared electrodes. The decrease in the phenol concentration with time indicates that the different Pt- and Ru-doped Ti/SnO_2-Sb anodes (Fig. 1a-c) as well as the Ti/RuO_2 one (Fig. 2a) are active for phenol degradation in the whole range of the studied current densities and alkaline conditions. In general, the higher the current density the faster the phenol-concentration decays. Nevertheless, notable differences can be distinguished concerning the anode composition. In the case of Ti/SnO_2-Sb-Pt electrode (Fig. 1a) the concentration of phenol is reduced down to 75 % for 24 h of electrolysis at 10 mA cm^{-2}, while at higher current densities the oxidation reaction is complete even at much shorter times. The Ti/RuO_2 anode is also capable of entirely eliminating the phenol from the simulated wastewater within 24 h, but higher current densities or longer electrolysis times are needed to achieve such a removal efficiency (Fig. 2a). The partial substitution of Sb by Ru in the tin dioxide lattice is detrimental to the electrode response towards the oxidative removal of phenol (Fig. 1b and 1c). At best, about 85 % phenol removal efficiency is achieved at 100 mA cm^{-2} and 24 hours of electrolysis for the Ti/SnO_2-Sb(9.75)-Pt-Ru(3.25) anode (Table 1), whereas the efficiency decreases down to 35-38 % after 24 hours of reaction for the Ti/SnO_2-Sb(3.25)-Pt-Ru(9.75) electrode, with little influence of the applied current density. In stark contrast, highly stable Ti/Co_3O_4 anodes show very low activity for phenol oxidation at the studied conditions (Fig. 2b and Table 1).

A more detailed inspection of curves in Fig. 1 reveals that the normalized concentration of phenol follows two well-defined time decay regimes, namely, a linear decrease (Zone I) to a certain transition or critical time or phenol conversion from which the time dependence becomes exponential (Zone II) (see an example and the corresponding kinetic equations in Fig. 2c). This kind of time dependence has been predicted by a theoretical kinetic model developed by Comninellis et al. [17,18,31,32] for the electrochemical mineralization of organic matter at BDD, as a model material for an ideal non-active anode. Briefly, the model assumes that organic matter undergoes a fast, mass-transport governed,

reaction with highly reactive hydroxyl radicals electrogenerated and adsorbed on the electrode surface from water (or hydrated hydroxyl ions in alkali) discharge. When the electrolysis is performed in an electrochemical reactor operated in batch recirculation mode under galvanostatic conditions, two kinetic regimes can be distinguished depending on the applied current density, j_{app} (see Appendices in Supp. Info.): a pseudo zero-order kinetics region of constant rate and 100 % current efficiency when $j_{app} < j_{lim}$ (limiting current density) and a pseudo first-order kinetics region with an exponential decay of COD with time and current efficiency below 100%. This model has been also used to predict the time changes in the concentration of single organic species during electrolysis on BDD [19].

On the contrary, non-active transition metal oxide anodes have shown experimentally to electro-oxidize refractory organic matter at a current efficiency below 100 % because of the competition of the OER, even within the zero-order regime [10,12,31]. These findings evidence that the performance of these anodes deviates from what is expected for an ideal non-active electrode. Thus, a generalized kinetic model, valid for both ideal and non-ideal non-active electrodes, can be easily derived from the Comninellis' model by introducing a zero-order or initial current efficiency, CE_0, that can be regarded as a deviation factor from the ideal behavior. This modification is done in order to recognize the influence of competing electron-consuming reactions under all electrolysis conditions (i.e. at all applied currents). The development of the generalized model and the relevant kinetic equations, jointly with the definition of the kinetic rate constants and efficiency parameters can be all looked up in the Appendices (Supp. Info).

The plots of $[Ph]/[Ph]_0$ or $\ln([Ph]/[Ph]_0)$ as a function of time showed straight lines with $R^2 > 0.99$ for all the studied samples. The zero-order (k_0, mol $m^{-3}s^{-1}$) and the first-order (k_1, s^{-1}) rate constants were estimated at different current densities from the slopes of these linear fittings, respectively, and they are summarized in Table 1. As it can be seen, the k_0 and k_1 values of the Ti/SnO_2-Sb(13-x)-Pt-Ru(x) (x=0.0, 3.25) and Ti/RuO_2 anodes increase with the current density, which indicates that phenol conversion is faster at the higher current densities. The anodes with composition Ti/SnO_2-Sb(3.25)-Pt-Ru(9.75) show

a distinct behavior, with k_0 being rather insensitive to the current density and hence reaching very similar phenol removal efficiencies. In the case of Ti/Co_3O_4 electrodes, the rate constants are remarkably low.

Despite correlation coefficients being close to unity for all studied electrode materials, our proposed kinetic model is only rigorously valid for Ti/SnO_2-Sb(13-x)-Pt-Ru(x). Anodes with nominal Ru content x=3.25 and 9.75 at % showed full zero-order behavior during the electrolysis course. Only Ti/SnO_2-Sb-Pt electrodes exhibited transition times from zero- to first-order kinetic regions being shortened with the increasing current density. This is the trend predicted by the model, considering that the phenolate conversion at which the condition $j_{Ph}=j_{lim}$ (where $j_{Ph}=CE_0 j_{app}$ is referred to as the effective current density employed to oxidize phenolate) is fulfilled should occur earlier as the current density rises, with the limiting case showing first-order behavior from the beginning of the electrolysis [19]. In contrast, Ti/RuO_2 electrodes showed first-order kinetics at low current densities (exponential concentration decay) and a linear to exponential transition in the phenol concentration vs. time plot at the higher current densities. One should recall, nonetheless, that these electrodes are active metal oxide anodes that follow a different oxidation mechanism in which the selective and partial oxidation of organics is favored [30-32]. An additional factor that could be involved in the observed discrepancies is the parallel formation of surface fouling products that is not taken into account in the developed kinetic model. Polymeric/oligomeric material formed via phenoxy radical reactions [14,30-32], especially in alkaline conditions, may block to a greater or lesser extent the electroactive area of the metal oxide film by the formation of hydrophobic domains that hinder the access of “fresh” phenolate or other soluble degradation products to the electrode surface. The formation of such fouling films is particularly important in active metal oxide anodes like Ti/RuO_2 (see Supporting Information).

In order to analyze the efficiency of the electrodes during the electro-oxidation treatments, two current efficiency parameters were considered, such as the above-mentioned zero-order current efficiency,

CE_0 and the total current efficiency, *TCE* [31]. CE_0 can be deduced from the apparent zero-order rate constant (k_0):

$$k_0 = \frac{CE_0}{n}\frac{I}{FV} \quad (1)$$

while *TCE* can be expressed as follows:

$$\frac{TCE}{n} = \frac{FV\left([Ph]_0 - [Ph]_f\right)}{I\tau} \quad (2)$$

where *I* is the applied current (A), *V* is the electrolyte volume (m^3), *F* is the Faraday constant (96485 C mol^{-1}), *n* is the number of electrons involved in the oxidation process, $[Ph]_0$ and $[Ph]_f$ are the initial and final concentrations of phenolate, and τ is either the time elapsed to the complete elimination of phenol or the total duration of the electrolysis (s). Because the mechanism of phenol oxidation is complex and not yet fully understood [12,14], *n* is unknown. Therefore, only the parameters expressed per electron transferred in the phenolate oxidation process (CE_0/n and *TCE/n*) can be estimated.

The results (Table 2) clearly indicate that the Ti/SnO_2-Sb-Pt anode displays the highest current efficiency for phenolate removal, and that Ti/RuO_2 shows very similar efficiencies to those for the Ru doped Ti/SnO_2-Sb-Pt electrodes with x=3.25 at. %. Upon increasing the Ru doping level in the SnO_2 matrix up to x=9.75 at. %, the current efficiency decreases. Finally, Ti/Co_3O_4 anodes show very low current efficiencies in accordance with their extremely poor activity for phenol oxidation.

Generally speaking, total and zero-order current efficiencies are similar to each other at low current densities, because the electrochemical oxidation is dominated by the zero-order kinetic regime. Thus, there is no difference between *TCE*/n and CE_0/n in Ru-doped Ti/SnO_2-Sb-Pt electrodes because they only show zero-order kinetics. As the first-order kinetic regime becomes more important at higher current densities, CE_0/n becomes higher than *TCE*/n.

The current efficiency is a measure of the electrical charge used for the anodic oxidation of phenolate versus the total electrical charge passed through the cell. Hence, the low *CE/n* values for the as-prepared anodes reveal the high refractory chemical nature of phenolate molecules and/or the

prevalence of the competing OER, which reduces the overall efficiency for the oxidation of phenolate. The significance of this by-reaction was confirmed by the progressive decrease in *CE/n* with the rise in current density for all the studied electrodes. These results indicate that the increase in current density leads to a significant acceleration of phenolate degradation, but the efficiency of water oxidation (OER) gradually increases at the expense of that of phenolate degradation reaction.

3.2. COD removal analysis

Because the electroxidation of phenolate can originate different intermediates [12,14], involving a distinct number of electrons, oxidation state and toxicity, the analysis of COD removal provides a better understanding and measure of the non-selective decontamination process, as well as a more precise evaluation of its efficiency. As it can be seen in Figures 3 and 4, the evolution of normalized COD with time and current density for the studied electrodes is quite similar to that observed for phenolate in Fig. 1 and 2. Briefly, the COD removal degree follows the trend Ti/SnO_2-Sb-Pt > Ti/RuO_2 ≈ Ti/SnO_2-Sb(9.75)-Pt-Ru(3.25) > Ti/SnO_2-Sb(3.25)-Pt-Ru(9.75) >> Ti/Co_3O_4, and, except for the mixed oxide with x = 9.75 % Ru (Fig. 3c), the removal efficiency increases with the current density.

A comparison of data in Figs. 1 and 2 with Figs. 3 and 4 makes it obvious that when phenolate concentration is zero the COD is not. This fact points out that phenol molecules were not completely oxidized to CO_2 and that some reaction intermediates remained in the solution. Nevertheless, and except in the case of Ti/Co_3O_4 anodes, the electro-oxidation treatment is capable of reducing between 20 % and 85 % of COD in 24 hours (Table 3), depending on the electrode and the current density, demonstrating its effectiveness in the removal of phenol from alkaline solution.

As for phenolate, the removal of COD decreases linearly and/or exponentially with time, depending on the current density and the nature of the electrode, so it can be also predicted with similar kinetic equations (Fig. 4c). Again, a simple modification of the kinetic model developed by Comninellis et al. [17,18] for the electrochemical mineralization of organic matter can be made to make it extensive to the

behaviour of non-active metal oxide anodes with performance departing from the ideal case. As in the preceding section, the modification basically consists of recognizing that even under zero-order conditions the oxidation of organic matter may suffer competition from undesired side reactions, like the OER. A zero-order current efficiency, CE'_0, for the elimination of COD (non-selective mineralization of organic matter) is defined that can also be regarded as a factor measuring the deviation with respect to the ideal performance. The relevant equations are described in detail in the Appendix B of Supp. Info.

As before, excellent fitting of experimental data to the kinetic equations predicted by the model were obtained with correlation coefficients better than 0.99. The values of the rate constants determined from the slopes of the straight lines (COD/COD_0 vs. *t* and $\ln(COD/COD_0$ vs. *t* plots) for each electrode are summarized in Table 3. It can be observed that, regardless the kinetics of the reaction (k'_0 and k'_1), the degradation rate increases with the current density, except in the case of Ti/SnO_2-Sb(3.25)-Pt-Ru(9.75) in which the rate remains nearly constant and independent on the applied current, in accordance with the results obtained for the electro-oxidation of phenolate (Table 1). Interestingly, best fittings for active Ti/RuO_2 anodes are of the first-order kind in all the electrolysis, although with correlation factors of about 0.98. Fittings for Ti/Co_3O_4 are poor (with correlation factors of about 0.8) and therefore the significance of the kinetic parameters is doubtful.

Contrary to the case when the phenolate removal was monitored (section 3.1), four electrons are exactly consumed for each oxygen molecule incorporated in the organic compound, so the molar ratio between the degraded molecule and the electrons consumed in the oxidation reaction can be accurately determined. Therefore, the current efficiency determined from COD removal provides a more practical parameter to evaluate the extent of phenolate electrochemical degradation. The current efficiency of COD removal (*ICE*') can be determined from experimental COD vs. time data according to the following equation:

$$ICE' = -\frac{4FV}{I}\frac{dCOD}{dt} \approx \frac{4FV(COD_t - COD_{t+\Delta t})}{I\Delta t} \quad (3)$$

where all the variables and constants have their usual meanings and COD is the chemical oxygen demand expressed in mol O_2 m^{-3}.

According to the generalized COD removal model, a constant value of the COD current efficiency is expected in the zero-order region, while it should decrease exponentially within the first-order region. The value of CE'_0 can be derived from k'_0 obtained from the linear fitting of the normalized COD vs. time data in the zero-order regime as follows:

$$k'_0 = \frac{CE'_0}{4}\frac{I}{FV} \tag{4}$$

where CE'_0 is the constant zero-order current efficiency for COD elimination and the other symbols have their usual meanings and unities.

Other current-efficiency related parameters of practical significance to assess and compare the performance of an electrochemical process for decontamination of waste waters polluted with organic matter are the total COD current efficiency, *TCE'*, and the time-averaged current efficiency, also known as electrochemical oxidation index, *EOI*:

$$TCE' = \frac{4FV\left(COD_0 - COD_f\right)}{I\tau} \tag{5}$$

$$EOI = \frac{\int_0^\tau ICE' dt}{\tau} \tag{6}$$

Where COD_0 and COD_f are the initial and final (after 24 h of electrolysis) chemical oxygen demand and τ is the duration of electrolysis. The electrochemical oxidation index is a more accurate measure of the average current efficiency than *TCE'* and it is usually used as a key parameter for comparison purposes among different research works.

All three current efficiency parameters are listed together in Table 4 for the different anodes employed in this work. At low current densities *TCE*' of Ti/SnO_2-Sb-Pt is close to 20 %, and that attained with the other electrodes containing Ru is between 5-10 %. These current efficiency values are between 20 and

10 times higher than those reported in Table 2, calculated just from phenolate concentration decay, showing that the number of electrons transferred from these electrodes to one molecule of phenolate is much higher than one, ranging between 20 and 10. These results emphasize the high activity of the studied electrodes towards phenolate electro-oxidation. However, the *TCE*' values for these anodes generally decrease with the applied current density, probably because an increasing degree of competition of parallel reactions (OER), to converge at rather similar low values at j_{app}>75 mA cm^{-2}. It is worth mentioning that the mixed oxide with x = 3.25 at% shows a quite similar performance to that of Ti/RuO_2, especially at low current densities. A higher level of Ru doping leads to a notable decrease in the current efficiency for COD removal. The low efficiencies obtained with the Ti/Co_3O_4 electrode (Table 4) confirm its poor activity for this reaction.

The calculated *EOI* values listed in Table 4 are very similar to those reported in the literature [11,12,25,26] and they follow the same dependence with current density and electrode composition than those observed for *TCE*'. Zero-order current efficiencies, CE'_0, also follow the same tendencies. Moreover, all three parameters are almost identical to each other at low current densities, or whenever the zero-order behavior predominates throughout the electrolysis process. On the contrary, CE'_0 remains higher than *TCE*' and *EOI* at the highest current densities or whenever the first-order kinetic behavior is dominant. Under such conditions, CE'_0 describes the performance at the initial stages of electrolysis, while the other two parameters are a better account for the efficiency of the overall process.

The evolution of the *ICE*' curves with time notably depends on the nature of the anode material and the current density. The *ICE*' vs. time curves for the Ti/SnO_2-Sb-Pt and Ti/RuO_2 anodes are shown in Figure 5. These plots display data point calculated according to approximate Eq (3) and simulated model predictions using fitting parameters derived from normalized COD data. With the only exception of points at the very beginning of electrolysis, all calculated *ICE*' points lie within the simulated curves for Ti/SnO_2-Sb-Pt (Fig. 5a). The deviations found at the initial stages of the electrochemical treatments

probably arise from the approximate nature of the *ICE*' calculation method. In agreement with the discussion made on the basis of the kinetic rate constants (Table 3), the electrochemical COD removal from phenol solutions proceeds under current control (constant *ICE*'=*CE*'$_0$ and zero-order kinetics) at the lowest current density. Upon increasing the applied current density, a mixed behavior with transition from constant (zero-order kinetics) to exponentially decaying *ICE*' (first-order kinetics) is observed. Finally, full mass transport limitation applies at the highest current density, with no constant *ICE*' region. Overall, the *ICE*' decreases with the increasing current density, which highlights the increasing predominance of the OER, as the main current-consuming side reaction. By contrast, the *ICE*' curve for the Ti/RuO_2 electrode (Fig. 5b) does not exhibit the ICE constant period, but a continuous decay throughout all the experiments independently of the current density. However, the agreement between calculated data points and simulated curves is poor, except at long electrolysis times. Again, it appears clear that the proposed model is too simplified to provide an accurate description for the electrochemical degradation of organic pollutants at active metal oxide anodes, especially those that favor the extensive formation of blocking polymeric films.

3.3. Degradation of intermediates

According to the literature, benzoquinone (BQ) is one of the main products formed during the electro-oxidation of phenol in aqueous solutions and its subsequent degradation by ring cleavage leads to the formation of several small organic acids [12,14,59]. In fact, the formation and destruction of quinone-like products has been considered as a direct evidence of the effective degradation of phenol to more biodegradable (less-toxic) residues [56]. The formation and subsequent evolution of this type of intermediates was monitored by UV-Vis spectroscopy. As shown in the example of Figure 6a, the initial UV spectrum of the alkaline phenolic solution presents two absorbance bands centered at 231 nm and 286 nm that are characteristic of phenolate anions. The intensity of both bands decreases with electrolysis time due to phenol electro-oxidation. At the same time, two new bands centered at 266 nm

and 319 nm are formed. The wavelength of these bands coincided with those observed in a freshly-prepared *p*-benzoquinone alkaline solution (Supp. Info), and therefore they can be attributed to the formation of *p*-benzoquinone during the course of the electro-oxidation process.

The BQ bands were detected in phenolic solutions treated by the different anodes, confirming the occurrence of phenolate oxidation with the formation of BQ as one of the main intermediates. In the case of Ti/SnO_2-Sb-Pt anode, Figure 6b shows that the concentration of BQ progressively increases with the electrolysis time to reach a maximum value and subsequently decreases. Since the instantaneous BQ concentration results from a balance between BQ electro-generation and its further electro-oxidation, the observed maxima can be explained in terms of an initially slower and subsequently faster electrochemical degradation rate of BQ. In agreement with the tendencies for phenolate electro-oxidation (Figs. 1 and 2) and COD removal (Figs. 3 and 4), the BQ concentration maxima shift towards shorter times as the applied current density is raised, as a result of the faster electrochemical conversion of phenolate into BQ.

Quite similar tendencies are also observed for the other electrodes (Figure 7), although some important differences can be pointed out. When using the Ti/RuO_2 anode, the maximum BQ concentrations (Fig. 7c) were always higher than in the case of Ti/SnO_2-Sb(13-x)-Pt-Ru(x) ones (Figs. 6b, 7a and 7b). The highest BQ concentrations obtained with this electrode arise from its higher capability to produce selective oxidation of organic matter to partially degraded products, instead of promoting their further oxidation until complete mineralization, both being characteristic properties of the so called “active” MOx anodes [30-32,59]. Then, the substitution of Sb by Ru in the Ti-SnO_2-Sb-Pt electrode should be expected to favor the formation of larger amounts of BQ intermediate and/or delay its removal, so that maxima of BQ concentration are difficult to be achieved within the analyzed treatment times (Fig. 7a and 7b). On the other hand, the Ti/Co_3O_4 anode (figure not shown) generated almost no BQ, what is in agreement with its low phenolate electroxidation activity.

3.4. Energy consumption and stability considerations

To now, the comparison of the electrodes has been carried out by considering only their electroxidation performance in terms of activity, kinetics, and current efficiency. However, the feasibility and potential utilization of the prepared electrodes, as an alternative to other anode-materials for the treatment of phenolic wastewaters, may rely on other more practical and/or economical parameters and aspects. In this sense, the reported electro-oxidation performance of the anodes must be more practically described by energy efficiency criteria. On the other hand, the anode stability and the cost of fabrication are also very important factors that must be taken into account when designing anode materials for wastewater remediation.

Table 5 summarizes the specific energy consumption (*EC)* values necessary for phenol elimination (not necessarily involved in complete mineralization) and COD removal contained in the simulated alkaline wastewater; and the service life of the electrodes (as previously determined in accelerated tests in 1 M NaOH [54]). The *EC* values, expressed in kWh kg^{-1} of either removed phenol (EC_{Ph}) or COD (EC_{COD}) were calculated with the use of the following equations [31]:

$$EC_{Ph} = \frac{\tau U I_{app}}{\Delta[Ph] V} \frac{1}{M_{Ph}} \quad (7)$$

$$EC_{COD} = \frac{\tau U I_{app}}{\Delta COD\, V} \frac{1}{M_{O_2}} \quad (8)$$

Where *U* is the cell voltage (V), I_{app} is the constant applied current (A), τ is either the time consumed to the total removal of phenol/COD or the total duration of electrolysis (h), Δ[Ph]/COD are the change in phenol concentration/COD (mol m^{-3}), V is the electrolyte volume (m^3) and *M* refers to the molar mass of either phenol or molecular oxygen (g mol^{-1}).

The lowest *EC* values for the as-prepared electrodes (Table 5) were generally obtained for the lowest current densities used in this work, in agreement with the trends in current efficiency (Table 2). The best energetic performance is that presented by the Ti/SnO_2-Sb-Pt electrode at a current density of 10

mA cm^{-2}. Unfortunately, it shows a considerably lower stability than the other anodes, thereby requiring of more frequent replacement upon continuous using. On the contrary, the Ti/RuO_2 electrode is very stable in alkaline conditions and displays relatively low energy consumption for phenolate electro-oxidation. However, it is much more expensive than all the other alternatives taking into account the high amount of ruthenium needed for its preparation. Finally, the spinel-like Ti/Co_3O_4 anode displays the highest stability in alkaline medium (Table 5), but it shows exceedingly high *EC* values that makes it unsuitable for practical application, in accordance with its very low activity for phenolate degradation and COD removal (Figures 3 and 4).

The properties of Ru doped Ti/SnO_2-Sb(13-x)-Pt-Ru(x) anodes (x = 3.25 and 9.75 at%) fill the gap between those of Ti/SnO_2-Sb-Pt and Ti/RuO_2 ones. They show 2 and 5 times longer service life than the anode made without Ru, respectively, and, although less stable, they are considerably cheaper than Ti/RuO_2. Moreover, these electrodes exhibit comparable responses in terms of energy consumption at low current densities. Particularly, the electrode with the lowest Ru content (x = 3.25 at%), gather an advantageous combination of enough stability, and relatively low energy consumption up to a current density of 25 mA cm^{-2}, as well as a poor activity for benzoquinone accumulation and electropolymerization.

The *EC* values obtained with Ti/SnO_2-Sb(13-x)-Pt-Ru(x) anodes are much better than those reported by other authors in more diluted neutral solutions. Yabuz et al. reported an *EC* of 290 kW h kg^{-1}_{Ph} for the electro-oxidation of a 200 ppm Ph/0.1 M Na_2SO_4 solution, with a Ti/RuO_2 electrode, at 15 mA cm^{-2} [56]. In another work, Zhang et al. reported an *EC* value of 233.1 kWh kg^{-1}_{Ph} for a combined photocatalytic-electrochemical oxidation treatment (UV-lamp of 8 W and j = 30 mA cm^{-2}) of a 50 ppm Ph/0.3 g L^{-1} NaCl solution, by using a Ti/RuO_2-Pt electrode [60]. On the other hand, the best results of energy consumption for COD removal, in the order of EC_{COD} = 40-200 kW h kg^{-1}_{COD}, are similar to those obtained by the highly efficient but much less stable SnO_2-Sb anodes [10]. Hence, the studied

Ti/SnO_2-Sb(13-x)-Pt-Ru(x) anodes offer contrasted advantages and great potential for the treatment of alkaline phenolic wastewaters.

4. Conclusions

The general electrochemical performance of Ti/SnO_2-Sb(13-x)-Pt-Ru(x) anodes towards phenolate elimination has been analyzed and compared to those of conventional Ti/RuO_2 and Ti/Co_3O_4 anodes, in order to evaluate their feasible application for decontamination of alkaline phenolic wastewaters. Among the studied anodes, the Ti/SnO_2-Sb-Pt electrode exhibits the best electroactivity, fastest kinetics and highest current efficiency for phenolate and benzoquinone by-product degradation, as well as COD removal. Its performance is remarkably better than that of the conventional, much more expensive, Ti/RuO_2 anode, and that of Ti/Co_3O_4 one, which shows a poor overall response. However, for practical application the service life of the Ti/SnO_2-Sb-Pt anode is considerably shorter than those of conventional ones. In this work, we demonstrate that the introduction of a small amount of Ru (3.25-9.75 at%) causes a remarkable increase in the stability of the electrode, but only a slight loss of its electrocatalytic performance and a small price increment. Thus, taking into account all relevant criteria (current efficiency, energy consumption, stability and cost), the Ti/SnO_2-Sb(9.75)-Pt-Ru(3.25) electrode seems to be the most promising anode material for the electrochemical treatment of alkaline phenolic wastewaters.

In terms of kinetics and efficiency, the results generally indicate that the increase in the applied current density leads to a significant acceleration of phenolate and p-benzoquinone degradation and COD removal, but also to an enhanced efficiency for the OER. This provokes a general decay of the current efficiencies and an increase in the energy consumption necessary to eliminate a given amount of phenolate. The obtained results suggest that the rates of phenolate and COD removal at Ti/SnO_2-Sb(13-x)-Pt-Ru(x) are under current control at the early stages of the electrochemical process, and they become mass-transport limited beyond a certain transition or critical time. However, experimental data

for Ti/RuO_2 and Ti/Co_3O_4 do not fit this kinetic model because they behave as active anodes and obey a different mechanism for the electrochemical oxidation of organic matter. Moreover, extensive oligomeric/polymeric film formation in these latter electrode materials is a further complication to the reaction mechanism that contributes to the deviations from the proposed kinetic model.

5. Acknowledgments

Financial support from the Spanish Ministerio de Economía y Competitividad and FEDER funds (MAT2013-42007-P, IJCI-2014-20012) and from the Generalitat Valenciana (PROMETEO2013/038) is gratefully acknowledged.

6. References

[1] Appendix A to Part 423 - 126 Priority Pollutants, in Code of Federal Regulations (United States). Title 40 - Protection of Environment. Vol. 29, 2014.

[2] Priority substances under the Water Framework Directive. European Commission. http://ec.europa.eu/environment/water/water-dangersub/pri_substances.htm (last updated: 19/11/2015)

[3] Toxicological review of phenol (EPA/635/R-02/006) (2002) U.S. Environmental Protection Agency.

[4] A. Hirata, M. Noguchi, N. Takeuchi, S. Tsuneda, Water Sci. Technol. 38 (1998) 205-212.

[5] B. Okolo, C. Park, M.A. Keane, J. Colloid Interface Sci. 226 (2000) 308-317.

[6] S. Esplugas, J. Giménez, S. Contreras, E. Pascual, M. Rodríguez, Water Res. 36 (2002) 1034-1042.

[7] J. Yu, P.E Savage, Appl. Catal. B: Environ. 31 (2001) 123-132.

[8] P. W. Cains, L. J. McCausland, A. R. Fernandes, P. Dyke, Environ. Sci. Technol. 31 (1997) 776.

[9] H.G. Oliveira, D.C. Nery, C. Longo, Appl. Catal. B: Environ. 93 (2010) 205-211.

[10] S. Stucki, R. Kotz, B. Carcer, W. Suter. J. Appl. Electrochem. 21 (1991) 99;

[11] C. Comninellis. Trans IChemE 70 (1992) 219-224.

[12] C. Comninellis, C. Pulgarin. J.Appl. Electrochem. 23 (1993) 108-112.

[13] Y.J. Feng, X.Y. Li, Water Res. 37 (2003) 2399-2407.

[14] X.Y Li, Y.H. Cui, Y.J. Feng, Z.M. Xie, J.D. Gu, Water Res. 39 (2005) 1972-1981.

[15] J.D. Rodgers, W.J. Jedral, N.J. Bunce, Environ. Sci. Technol. 33 (1999) 1453-1457.

[16] P. Cañizares, J. Lobato, R. Paz, M.A. Rodrigo, C. Sáez, Water Res. 39 (2005) 2687-2703.

[17] M.A. Rodrigo, P.A. Michaud, I. Duo, M. Panizza, G. Cerisola, Ch. Comninellis, J. Electrochem. Soc. 148 (2001) D60-D64.

[18] M. Panizza, P.A. Michaud, G. Cerisola, Ch. Comninellis, J. Electroanal. Chem., 507 (2001) 206-214.

[19] J. Iniesta, P.A. Michaud, M. Panizza, G. Cerisola, A. Aldaz, Ch. Comninellis, Electrochim. Acta, 46 (2001) 3573-3578.

[20] B. Adams, M. Tian, A. Chen, Electrochim. Acta 54 (2009) 1491-1498.

[21] F. Montilla, E. Morallón, J.L. Vázquez. J. Electrochem. Soc. 152 (2005) B421.

[22] M.E. Makgae, C.C. Theron, W.J. Przybylowicz, A.M. Crouch, Mat. Chem. Phys. 92 (2005) 559-564.

[23] M.E. Makgae, M.J. Klink, A.M. Crouch, Appl. Catal. B 84 (2008) 659-666.

[24] Y.Q. Wang, B. Gu, W.L. Xu, J. Hazard. Mat. 162 (2009) 1159-1164.

[25] M.A.M. Cartaxo, K. Ablad, J. Douch, Y. Berghoute, M. Hamdani, M.H. Mendonça, J.M.F. Nogueira, M.I.S. Pereira, Chemosphere 86 (2012) 341-347.

[26] R. Sripriya, M. Chandrasekaran, K. Subramanian, K. Asokan, M. Noel, Chemosphere 69 (2007) 254-261.

[27] D. Pletcher, F.C. Walsh, Industrial Electrochemistry, second ed., Chapman-Hall, London, 1990.

[28] K. Rajeshwar, J.G. Ibanez, Environmental electrochemistry: Fundamentals and Applications in Pollution Abatement, Academic Press Inc., San Diego, 1997.

[29] A. Fernandes, M.J. Pacheco, L. Ciríaco, A. Lopes, Appl. Catal. B Environ. 176-177 (2015) 183-200.

[30] G. Foti, D. Gandini, Ch. Comninellis, Current Topics Electrochem. 5 (1997) 71–91.

[31] C.A. Martínez-Huitle, S. Ferro, Chem. Soc. Rev. 25 (2006) 1324-1340.

[32] A. Kapałka, G. Fóti, Ch. Comninellis, in: Ch. Comninellis, G. Chen (Eds.), Electrochemistry for the Environment, Springer, New York, 2010, pp. 1-23.

[33] S.S. Block. Disinfection, Sterilization, and Preservation, fifth ed., Lippincott Williams & Wilkins, Philadelphia, 2001.

[34] A.D. McRae, Sewage Ind. Wastes, 31 (1959) 712-718.

[35] T.E. Short, B.L. DePrater, L.H. Myers, in: ACS Fuels Volumes (Fuel preprints of the ACS Energy and Fuels Division) 1974 Fall (ATLANTIC CITY) 19(5), pp. 113-148.

[36] J.M. Wong, Y.-T. Hung, in: L.K. Wang, Y.-T. Hung, H.H. Lo, C. Yapijakis (Eds.), Handbook of Industrial and Hazardous Wastes Treatment, second ed., Marcel Dekker, Inc., New York·Basel, 2004, pp. 144-216.

[37] Petroleum refining water/wastewater use and management. IPIECA Operations Best Practice Series (2010).

[38] L.K. Wang, N.K. Shammas, Y.-T. Hung, Waste Treatment in the Metal Manufacturing, Forming, Coating, and Finishing Industries, CRC Press, Boca Raton, 2008.

[39] B. Zacharias, R. Kayser. Treatment of a steel Works Effluent with a conventional Single-Sludge System Built in Cascades, p 705. Proceedings of the 50th Industrial Waste Conference (1995), by Purdue Research Foun. Ann Arbor Press.

[40] N.J. Bunce, D. Bejan, Electrochim. Acta 56 (2011) 8085.

[41] P. Cañizares, M. Díaz, J.A Domínguez, J. Lobato, M.A Rodrigo, J. Chem. Technol. Biotechnol. 80 (2005) 565.

[42] R. Berenguer T. Valdés-Solís, A.B. Fuertes, C. Quijada, E. Morallón, J. Electrochem. Soc. 155 (2008) K110.

[43] B.E. Conway, E. Ayranci, H. Al-Maznai, Electrochim. Acta 47 (2001) 705.

[44] R. Berenguer, J.P. Marco-Lozar, C. Quijada, D. Cazorla-Amorós, E. Morallón, Carbon 48 (2010) 2734;

[45] R. Berenguer, J.P. Marco-Lozar, C. Quijada, D. Cazorla-Amorós, E. Morallón, Energy Fuels 24 (2010) 3366.

[46] C. Comninellis, A. Nerini, J.Appl. Electrochem. 25 (1995) 23.

[47] D. Rajkumar, J. G. Kim, K. Palanivelu, Chem. Eng. Technol. 28 (2005) 98.

[48] S. Trasatti, in: J. Lipkowski, P.N. Ross (Eds.), The Electrochemistry of Novel Materials, VCH Publisher Inc., Weinheim, 1994, pp. 207–295.

[49] S. Trasatti, Electrochim. Acta 45 (2000) 2377.

[50] C. Comninellis, G. P. Vercesi, J. Appl. Electrochem. 21 (1991) 335.

[51] F. Vicent, E. Morallon, C. Quijada, J.L. Vazquez, A. Aldaz, F. Cases, J. Appl. Electrochem. 28 (1998) 607.

[52] F. Montilla, E. Morallón, A. De Battisti, J.L. Vázquez, J. Phys. Chem. B 108 (2004) 5036.

[53] H.Y. Ding, Y.J. Feng, J.W. Lu, Russ. J. Electrochem. 46 (2010) 72.

[54] R. Berenguer, J.M. Sieben, C. Quijada, E. Morallón, ACS Appl. Mater. Interfaces 6 (2014) 22778.

[55] R. Berenguer, C. Quijada, E. Morallón, Electrochim. Acta 54 (2009) 5230.

[56] Y. Yavuz, A.S. Koparal, J. Hazard. Mat. B136 (2006) 296-302.

[57] A. La Rosa-Toro, R. Berenguer, C. Quijada, F. Montilla, E. Morallón, J. L. Vázquez, J. Phys. Chem. B 110 (2006) 24021.

[58] R. Berenguer, A. La Rosa-Toro, C. Quijada, E. Morallón, J. Phys. Chem. C 112 (2008) 16945.

[59] C. Bock, B. MacDougall, J. Electroanal. Chem. 491 (2000) 48-54.

[60] F. Zhang, M. Li, W. Li, C. Feng, Y. Jin, X. Guo, J. Cui, Chem. Eng. J. 175 (2011) 349-355.

Tables and Figures

Table 1. Effect of current density and electrode composition on the pseudo zero-order (k_0, mol $m^{-3}s^{-1}$), pseudo-first-order (k_1, s^{-1}) rate constants and removal efficiency (%) for electrolysis of phenol in alkaline medium.

		10 mA cm^{-2}			25 mA cm^{-2}			50 mA cm^{-2}			75 mA cm^{-2}			100 mA cm^{-2}		
Electrode	(x)	10^4 k_0	10^5 k_1	Removal Eff.	10^4 k_0	10^5 k_1	Removal Eff.	10^4 k_0	10^5 k_1	Removal Eff.	10^4 k_0	10^5 k_1	Removal eff.	10^4 k_0	10^5 k_1	Removal eff.
Ti/SnO_2-	0.00	1.10	2.00	77.6	1.33	3.67	90.0	1.54	7.33	98.0	2.03	11.7	100	3.05	13.5	100
Sb(13-x)	3.25	0.46	-	34.5	0.87	-	65.0				0.95	-	72.6	1.11	-	85.2
-Pt-Ru(x)	9.75	0.35	-	36.1	0.46	-	37.7	0.43	-	35.1						
Ti/RuO_2		-	0.70	38.1	-	1.17	64.6	1.34	3.17	89.1	1.81	7.17	100	2.81	9.39	100
Ti/Co_3O_4		0.05	-	6.3	0.08	-	10.2	-	0.11	14.0						

Table 2. Zero-order current efficiency, CE_0/n, and total current efficiency, *TCE*/n, per electron transferred in the electro-oxidation of phenol in alkaline medium at different current densities.

		Current efficiency (%)									
		10 mA cm^{-2}		25 mA cm^{-2}		50 mA cm^{-2}		75 mA cm^{-2}		100 mA cm^{-2}	
Electrode	(x)	*TCE*/n	CE_0/n	TCE/n	CE_0/n	*TCE*/n	CE_0/n	*TCE*/n	CE_0/n	*TCE*/n	CE_0/n
Ti/SnO_2-Sb(13-x)-Pt-Ru(x)	0.00	0.92	1.07	0.42	0.51	0.23	0.30	0.22	0.26	0.23	0.29
	3.25	0.45	0.45	0.34	0.34			0.13	0.12	0.11	0.11
	9.75	0.35	0.33	0.18	0.18	0.08	0.08				
Ti/RuO_2		0.45	-	0.29	-	0.24	0.26	0.19	0.23	0.18	0.27
Ti/Co_3O_4		0.06	0.05	0.06	0.03	0.04	-				

Table 3. Effect of current density and electrode composition on the pseudo zero-order (k'_0, mol $m^{-3}s^{-1}$), pseudo first-order (k'_1, s^{-1}) rate constants and removal efficiencies for the elimination of COD in 1000 ppm PhOH/0.5 M NaOH.

		10 mA cm^{-2}			25 mA cm^{-2}			50 mA cm^{-2}			75 mA cm^{-2}			100 mA cm^{-2}		
Electrode	(x)	$10^4\ k'_0$	$10^5\ k'_1$	Removal Eff.	$10^4\ k'_0$	$10^5\ k'_1$	Removal Eff.	$10^4\ k'_0$	$10^5\ k'_1$	Removal Eff.	$10^4\ k'_0$	$10^5\ k'_1$	Removal eff.	$10^4\ k'_0$	$10^5\ k'_1$	Removal eff.
Ti/SnO_2-Sb(13-x)-Pt-Ru(x)	0.00	4.83	-	51.2	6.32	1.43	65.0	7.40	1.73	72.4	8.46	1.93	75.9	-	2.54	85.6
	3.25	2.63	-	19.7	3.97	-	42.2				4.84	-	51.0	6.19	0.94	55.2
	9.75	1.46	-	19.9	2.17	-	26.8	1.84	-	20.9						
Ti/RuO_2		-	0.35	27.4	-	0.54	37.6	-	0.88	52.7	-	1.20	65.3	-	1.58	73.9
Ti/Co_3O_4		0.13	-	6.7	-	0.30	10.7	-	0.30	14.0						

Table 4. Zero-order (CE'_0, %), total current efficiencies (TCE', %) and electrochemical oxidation index (EOI, %) for the elimination of COD in 1000 ppm PhOH/0.5 M NaOH at different current densities.

		10 mA cm^{-2}			25 mA cm^{-2}			50 mA cm^{-2}			75 mA cm^{-2}			100 mA cm^{-2}		
Electrode	(x)	CE'_0	TCE'	EOI	CE'_0	TCE'	EOI	CE'_0	TCE'	EOI	CE'_0	TCE'	EOI	CE'_0	TCE'	EOI
Ti/SnO_2-Sb(13-x)-Pt-Ru(x)	0.00	18.6	18.6	18.6	9.8	9.1	9.1	5.7	5.3	5.2	4.4	3.6	3.9	-	3.0	3.5
	3.25	10.1	7.5	10.2	6.1	6.4	7.7				2.5	2.6	2.7	2.4	2.1	2.5
	9.75	5.6	5.3	5.1	3.4	3.6	4.5	1.4	1.5	1.6						
Ti/RuO_2	-	-	10.0	11.5	-	5.4	6.5	-	3.8	4.3	-	3.2	3.6	-	2.7	3.2
Ti/Co_3O_4		1.4	2.3	3.8	-	1.4	1.9	-	1.0	1.4						

Table 5. Energy consumption (*EC*) for the removal of Ph and COD in the electrolysis of the simulated alkaline wastewater (1000 ppm Ph/0.5 M NaOH) for the as-prepared anode materials. Service life of the electrodes in the accelerated test performed at 0.5 A cm^{-2} in 1 M NaOH in the absence of phenol.

		EC_{Ph} (kW h kg^{-1}_{Ph})/ EC_{COD} (kW h kg^{-1}_{COD})										Service Life
Electrode	(x)	10 mA cm^{-2}		25 mA cm^{-2}		50 mA cm^{-2}		75 mA cm^{-2}		100 mA cm^{-2}		A h mg^{-1}
Ti/SnO_2-Sb(13-x)-Pt-Ru(x)	0.00	83	47	207	112	444	235	564	391	621	560	22
	3.25	174	112	286	162			1017	532	1380	783	63
	9.75	200	157	420	263	1193	803					106
Ti/RuO_2		151	81	279	184	496	359	705	509	883	663	181
Ti/Co_3O_4		629	324	1706	689	2914	1140					184

Figure 1. Evolution of the normalized phenolate concentration with time for (a) Ti/SnO_2-Sb-Pt; (b) Ti/SnO_2-Sb(9.75)-Pt-Ru(3.25); (c) Ti/SnO_2-Sb(3.25)-Pt-Ru(9.75) at different current densities (electrolyte = 1000 ppm Ph/0.5 M NaOH).

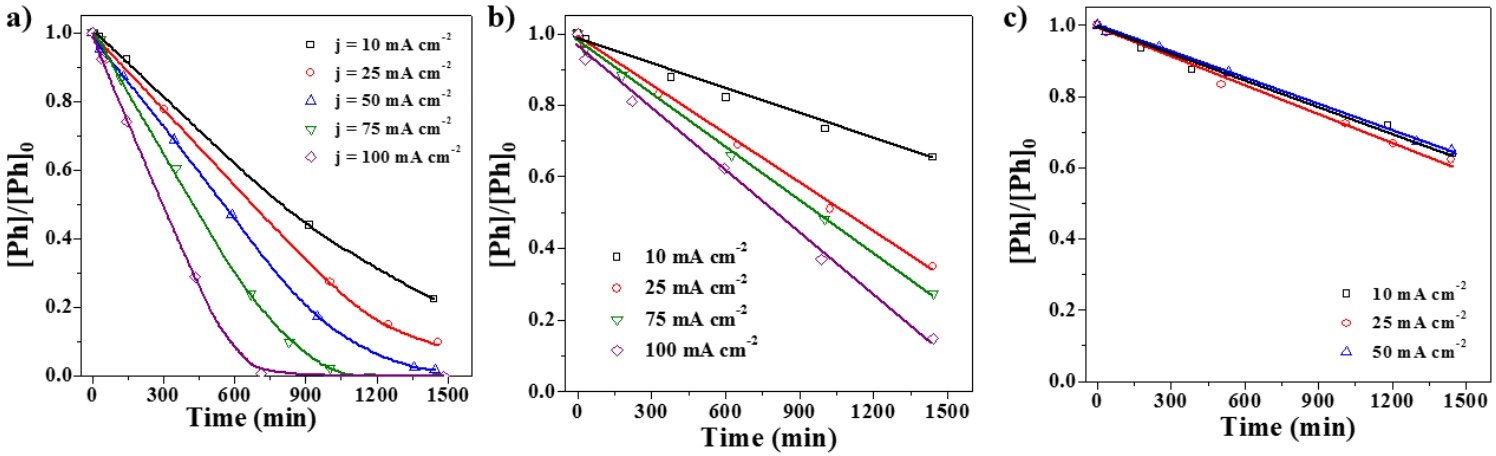

Figure 2. Evolution of the normalized phenolate concentration with time for (a) Ti/RuO_2 and (b) Ti/Co_3O_4 anodes at different current densities (electrolyte = 1000 ppm Ph/0.5 M NaOH); (c) simplified kinetic models for phenolate decay.

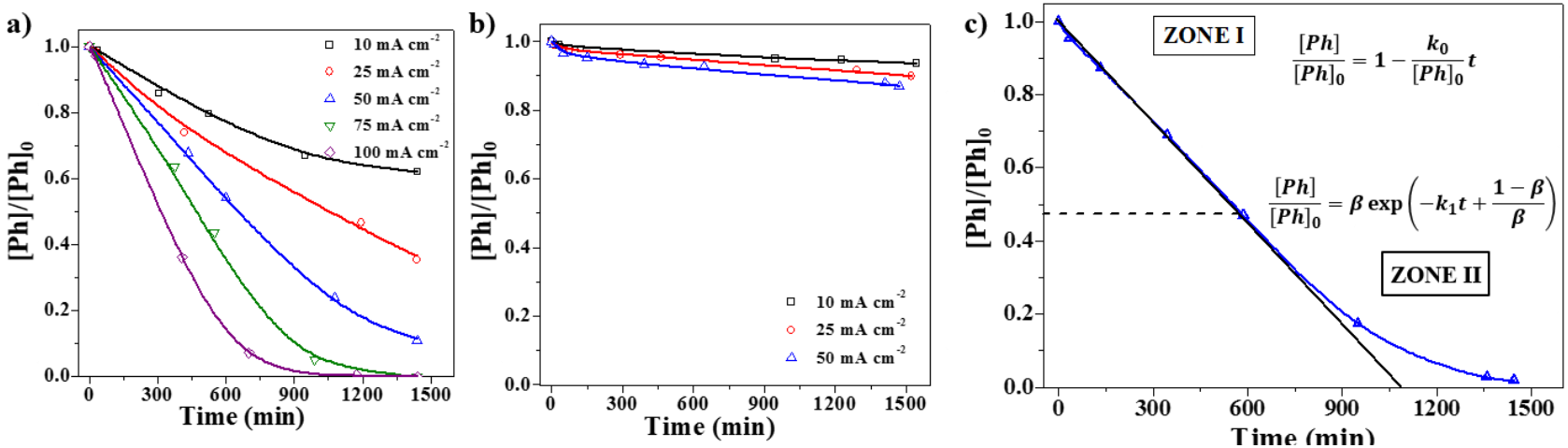

Figure 3. Evolution of normalized COD with time for (a) Ti/SnO_2-Sb-Pt; (b) Ti/SnO_2-Sb(9.75)-Pt-Ru(3.25); (c) Ti/SnO_2-Sb(3.25)-Pt-Ru(9.75) anodes at different current densities (electrolyte = 1000 ppm Ph/0.5 M NaOH).

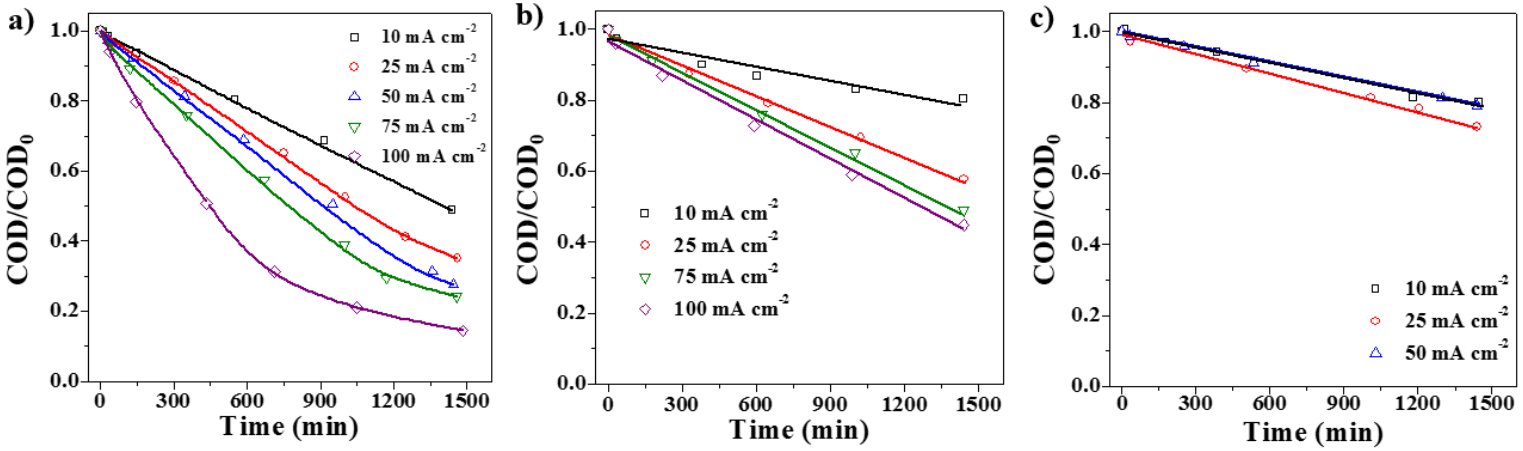

Figure 4. Evolution of normalized COD with time for (a) Ti/RuO_2 and (b) Ti/Co_3O_4 anodes at different current densities (electrolyte = 1000 ppm Ph/0.5 M NaOH); (c) simplified kinetic models for COD decay.

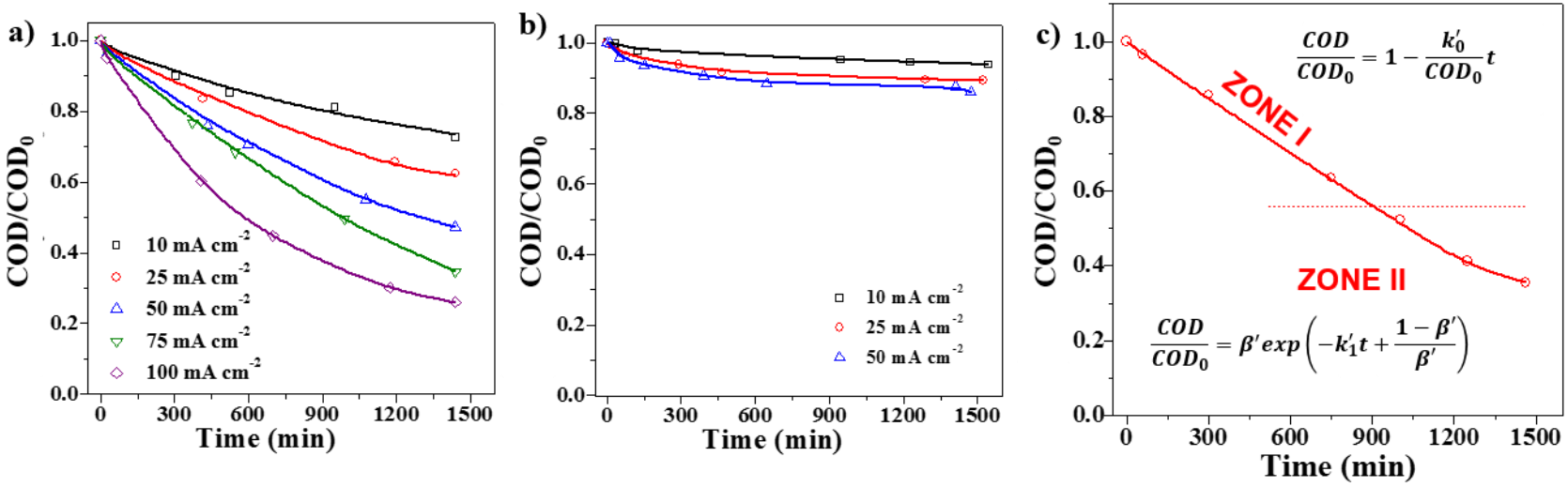

Figure 5. Evolution of the instantaneous current efficiency (ICE') with time for (a) Ti/SnO_2-Sb-Pt; (b) Ti/RuO_2 anodes at different current densities (electrolyte = 1000 ppm Ph/0.5 M NaOH). Open symbols represent calculated ICE' data and solid lines are the simulated model descriptions for ICE' based on fitting of experimental normalized COD data.

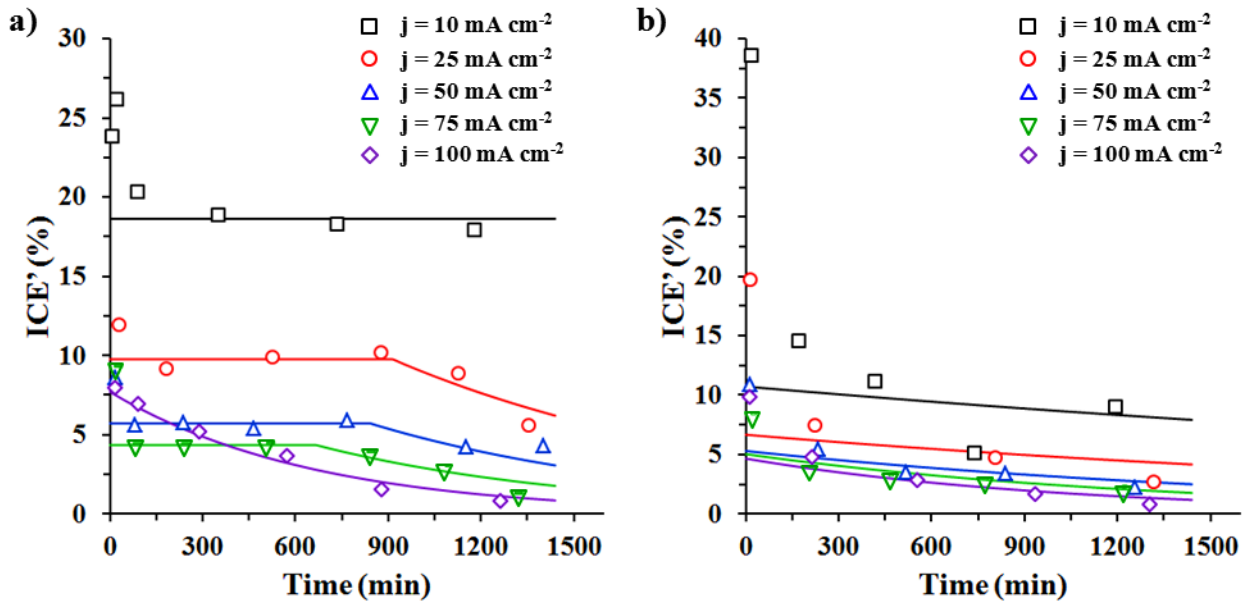

Figure 6. Evolution of (a) UV spectrum (100 mA cm^{-2}) and (b) benzoquinone concentration (at different current densities) with time during the electrochemical treatment of 1000 ppm Ph/0.5 M NaOH solution using Ti/SnO_2-Sb-Pt.

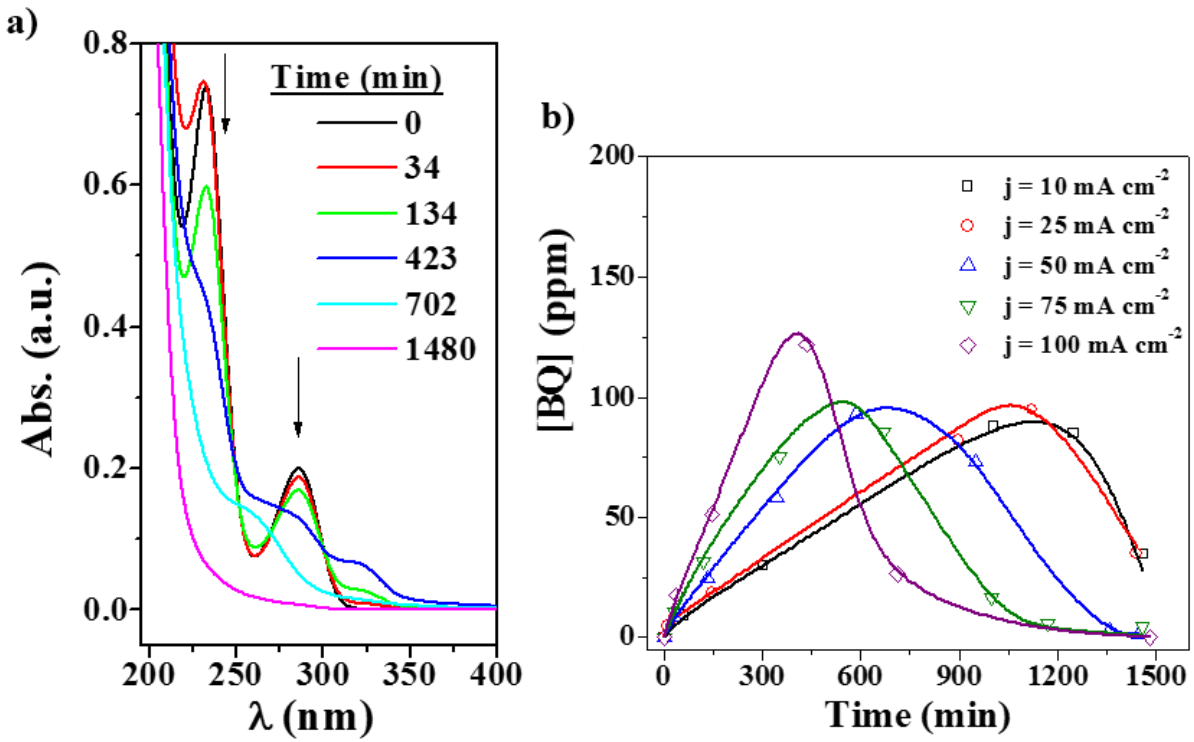

Figure 7. Evolution of benzoquinone concentration with time during the electrochemical treatment of 1000 ppm Ph/0.5 M NaOH solution at different current densities using (a) Ti/SnO_2-Sb(9.75)-Pt-Ru(3.25); (b); Ti/SnO_2-Sb(3.25)-Pt-Ru(9.75); and (c) Ti/RuO_2.

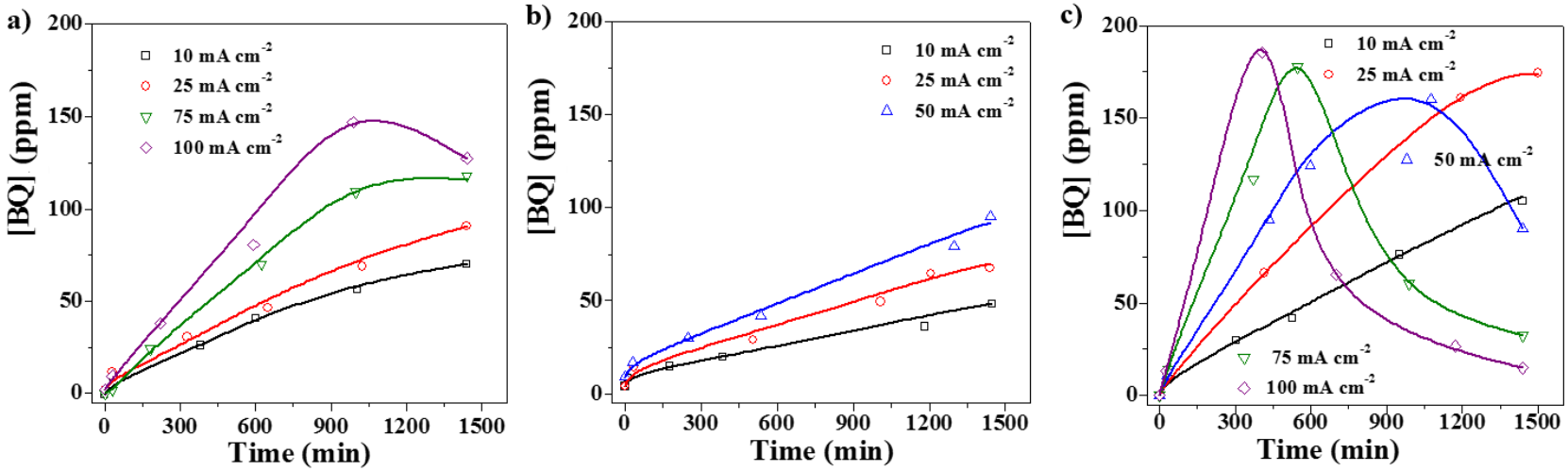

*Graphical Abstract

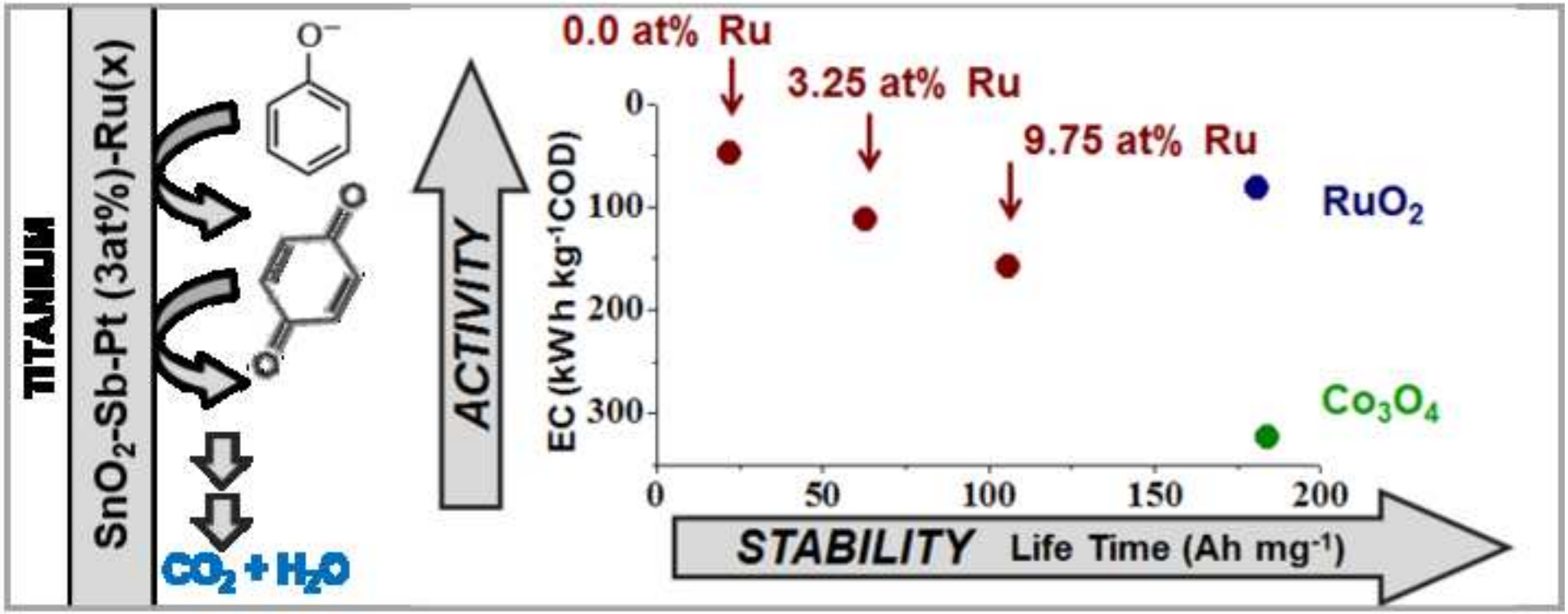

Research Highlights

Electrocatalytic degradation of phenol on Pt- and Ru-doped Ti/SnO_2-Sb anodes in an alkaline medium

R. Berenguer[a], J.M. Sieben[b], C. Quijada[c], E. Morallón[a,*]

[a] Departamento de Química Física and Instituto Universitario de Materiales, Universidad de Alicante, Apartado 99, E-03080 Alicante, Spain.
[b] Instituto de Ingeniería Electroquímica y Corrosión and CONICET, Universidad Nacional del Sur, Av. Alem 1253, (B8000CPB) Bahía Blanca, Argentina.
[c] Departamento de Ingeniería Textil y Papelera, Universidat Politècnica de València, Plaza de Ferrándiz y Carbonell, E-03801 Alcoy (Alicante), Spain.

* Corresponding author: morallon@ua.es

Highlights

• Pt/Ru-doped SnO_2-Sb anodes reduce 100% Ph and 85% COD from 1000 ppm Ph alkaline waste

• SnO_2-Sb-Pt(3at%) shows the best electroactivity, higher than RuO_2 and Co_3O_4 anodes

• A small Ru% enhances the stability of SnO_2-Sb-Pt, keeping good activity and low cost

• Energy consumption ranges between 80-600 kWh/Kg_{Ph} and 40-560 kWh/Kg_{COD} in best cases

• SnO2-Sb(13-x)-Pt(3at%) with $0 \leq x \leq 3.25$at%Ru are the most promising electrocatalysts

Supplementary Material

Click here to download Supplementary Material: Supplementary information.docx